AGRICULTURAL AND FOREST METEOROLOGY 149 (2009) 570–581

available at www.sciencedirect.com

ScienceDirect

journal homepage: www.elsevier.com/locate/agrformet

Decoupling structural and environmental determinants of sap velocity
Part II. Observational application

D. Dragoni [a,*], *K.K. Caylor* [b], *H.P. Schmid* [a,1]

[a] *Indiana University, Department of Geography, Bloomington, USA*
[b] *Princeton University, Department of Civil and Environmental Engineering, Princeton, NJ 08544, USA*

ARTICLE INFO

Article history:
Received 4 April 2008
Received in revised form
2 October 2008
Accepted 6 October 2008

Keywords:
Transpiration
Sap flux
Sap velocity
Sap conductance
Plant–water interactions
Soil moisture
Sugar maple
Acer saccharum

ABSTRACT

In this work we present experimental evidence in support of a new approach for investigating the dependence of sap velocity on atmospheric water demand and soil moisture supply. In this method, sap velocity is defined as the product of two components: the first describes the 'shape' of the radial profile of sap velocity, which is consistent through time and is likely linked to the species-specific anatomical and structural properties of the conducting xylem; the second, which we define as stem conductance, captures the time-dependent component of sap velocity that is mostly governed by shifts in atmospheric water demand and individual tree water supply. The heat pulse technique was used to estimate radial profiles of sap velocity and transpiration from a sample of 16 mature sugar maples (*Acer saccharum*) located along a topographic transect in a mixed deciduous forest. Our results demonstrate that: (1) stem conductance is strongly correlated with bulk air conditions (with confidence intervals for all the sampled trees greater than 99% and average R^2 of 0.43, 0.57, 0.54 for vapor pressure deficit (VPD), PPFD and net radiation, respectively) and atmospheric water demand (average R^2 equal to 0.73) on an hourly basis and that it is independent of tree size; (2) sensitivity of stem conductance to atmospheric water demand in sugar maples is also correlated to variation in local soil water availability (P-value = 0.014, R^2 = 0.43) which arises due to a mild topographic gradient (i.e. 20 m of relative relief along 140 m) and relatively shallow soil. Although the sampled trees were subjected to a wide range of atmospheric water demands and soil moistures, the response to changes in environmental conditions is entirely explainable by dynamics of stem conductance rather than the relative fraction of sap flow along the radial profile, as some of the previous studies reported. Overall, our results confirm our theoretical approach and the possibility of partitioning sap velocity variability between either xylem properties or changes in environmental conditions.

* *Corresponding author at*: 120 Student Building – Geography Department, Indiana University, 701 E Kirkwood Ave, Bloomington, IN 47405, USA. Tel.: +1 812 855 5557; fax: +1 812 855 1661.
E-mail address: ddragoni@indiana.edu (D. Dragoni).

[1] Currently at the Institute of Meteorology and Climate Research, Atmospheric Environmental Research Division, Research Center Karlsruhe (FZK/IMK-IFU) - 82467 Garmisch-Partenkirchen, Germany.

0168-1923/$ – see front matter
doi:10.1016/j.agrformet.2008.10.010

1. Introduction

The exchange of water between the atmosphere and biosphere is an important determinant of climate that also influences the productivity of vegetation, as transpiration links carbon, water and energy cycles (Jones, 1992). Investigations into the manner by which shifts in water supply and demand affect transpiration are thus critical to better understand water cycling in forest ecosystems. In particular, measuring transpiration at the scale of individual trees has the theoretical advantage of preserving vital information on important plant–environment functional links and flux partitioning between species and landscape heterogeneity (Loranty et al., 2008a; Meinzer et al., 2001; Oren et al., 1998; Wilson et al., 2001; Wullschleger et al., 2001).

Whole-tree transpiration has been estimated by means of sap flow probes (e.g., Granier, 1985; Green et al., 2003; Smith and Allen, 1996). In forest environments, sap flow approaches offer the dual advantages of practicality and repeatability of measurements. Furthermore, these techniques can provide critical insights into the effects of spatio-temporal shifts in environmental conditions on the temporal dynamic of sap flow, sap velocity and xylem properties in woody trees (Fiora and Cescatti, 2008; Ford et al., 2004b; Kubota et al., 2005; Kumagai et al., 2007). Critical for this task is the determination of the spatial distribution of sap velocities (v_s, $L\,T^{-1}$), which can vary greatly within the cross-section of the stem expressed in polar coordinates, with angular position θ and radial position (r) and time (t), so that the instantaneous sap flow for an individual tree (F_s, $L^3\,T^{-1}$) is

$$F_s(t) = \int_0^{2\pi} \int_0^R v_s(r;\theta;t) \cdot dr\, d\theta \quad (1)$$

where R is the radius of the xylem.

Obtaining a good description of the spatial distribution of sap velocity (v_s) can be challenging, especially for species such as sugar maples (*Acer saccharum*), which have deep active xylem that makes sampling sap velocities along the entire radius of the sapwood technically difficult. Several strategies have been proposed to interpolate and extrapolate sap velocities in the unknown portion of the xylem (Ewers et al., 2002; Hatton et al., 1990; Pausch et al., 2000; Poyatos et al., 2007). All of these methods rely either on simple proportionality rules (Ewers et al., 2002, 2007; Hatton et al., 1990; Pausch et al., 2000; Poyatos et al., 2007; Tang et al., 2006), or a strictly defined family of polynomial functions, usually linear (Bernier et al., 2002) or quadratic (Ford et al., 2004b).

While any of these techniques may be relatively successful in interpolating the actual radial profile of sap velocity, they all lack a general framework for investigating the link between observed variability in sap velocity and the spatio-temporal patterns of atmospheric water supply and demand. Of course, independent knowledge of the control exerted by water supply and demand on sap velocities is critical for determining how species composition, landscape heterogeneity, and shifts in environmental conditions each act to affect variability in transpiration (Cermak and Nadezhdina, 1998; Fiora and Cescatti, 2008; Kumagai et al., 2007; Loranty et al., 2008a). Moreover, clarification of the structural and environmental determinants of sap velocities would reduce uncertainty introduced by integrating short-term, individual observations of water use over larger spatial and temporal scales (Kumagai et al., 2007; Loranty et al., 2008b).

Recently, Ford et al. (2004b) used a 3-parameter Gaussian distribution to describe the radial profile of sap velocity in four different pine species. While confirming the importance of obtaining accurate descriptions of the radial profile of sap velocity, they also proposed the use of one of the parameters of the Gaussian function (β, in (Ford et al., 2004b)) to link the variability of the radial profile over time and among trees with changes in atmospheric vapor pressure deficit (VPD). In a similar study, Kubota et al. (2005) applied a Weibull function to interpolate radial sap velocity measurements in three Japanese beech (*Fagus crenata*) and investigate the effects of different environmental conditions on the '*shape*' of the radial profile.

However, because these techniques do not resolve the separate short-term (i.e. hourly or daily) and long-term (i.e. seasonal or annual) variability in sap velocity, these past approaches only allow for a partial investigation into how both the xylem structure/functionality and shifts in tree water use interact to determine sap velocity. For this reason, their results may still be affected by the spatial component of sap velocity variability that mainly originates from changes in morphology/phenology and xylem properties at the tree scale, and varies over much larger time periods than the one characterizing the hourly and daily dynamics in water supply and demand.

In Part I of this manuscript (Caylor and Dragoni, 2009), we redefine the instantaneous sap velocity v_s at any point $x = r/R$ in the radial profile as the product of a time-invariant sap velocity distribution $\rho_s(x)$ (unitless) and a new time-varying term which we define as the stem conductance $c_s(t)$ ($L\,T^{-1}$), so that

$$v_s(x,t) = \rho_s(x) \cdot c_s(t) \quad (2)$$

In Eq. (2), the quantity $\rho_s(x)$ describes the relative distribution of sap velocity over the relative radial coordinate bounded by $0 \le x \le 1$ such that $\int_0^1 \rho_s(x)\,dx = 1$. Our presentation in Part I of this manuscript provides compelling evidence that $\rho_s(x)$ could be assumed constant among trees of different sizes and under different environmental conditions, at least within a growing season. We speculate that the variability of $\rho_s(x)$ may be directly linked to changes in active xylem structure, which is determined by changes in tree phenology, structure and morphology that vary over seasons or years. In contrast, c_s describes the variability of sap velocity profiles directly linked to the rapid adjustments to water use caused by stomata regulation in response to hourly variability of water supply and demand. The observation that $\rho_s(x)$ can be constant over time both within and between trees allows us to focus our analysis in this presentation to c_s. Therefore, our goal in Part II is to further expand our analysis in Part I by investigating the link between c_s, which captures the time-varying component of sap velocity, and the spatio-temporal variability in bulk atmospheric/soil conditions that together determine individual tree water supply and demand. Our specific objectives are (1) to demonstrate that the dynamic of c_s is directly related to changes in atmospheric water demand and soil water supply

as predicted by the theoretical framework presented in Part I; and (2) to present evidence that the our approach can provide additional insights into the mechanisms and controls that regulate sap velocity and sap flow in trees.

2. Materials and methods

2.1. Theoretical framework

In Part I of this manuscript (Caylor and Dragoni, 2009) we propose the use of a Beta distribution function to describe $\rho_s(x)$ in Eq. (2), which in this case is defined as

$$v_s(x,t) = B_{PDF} \cdot c_s(t) = \left[\frac{1}{B(\alpha,\beta)}(x)^{\alpha-1}(1-x)^{\beta-1}\right] \cdot c_s(t) \quad (3)$$

where α and β are shape parameters that together determine the distribution of relative sap velocity across a radial profile, $B(\alpha, \beta)$ is the Beta function

$$B(\alpha,\beta) = \int_0^1 t^{\alpha-1}(1-t)^{\beta-1}dt \quad (4)$$

In addition, the radial location that contains the average value of the relative velocity profile, $\bar{\rho}_s$, is the average of the Beta distribution, which is given by

$$\bar{\rho}_s = \frac{\alpha}{\alpha+\beta} \quad (5)$$

So, in the case of circumferentially homogenous sap velocity, sap flow for the whole tree (F_s, $M\,T^{-1}$) can be estimated as the product of the sapwood area of the tree (A_s, L^2) and the average sap velocity $[\bar{v}_s(t) = \bar{\rho}_s c_s(t)]$ as

$$F_s(t) = 2 \cdot \bar{\rho}_s \cdot c_s(t) \cdot A_s = 2\pi R^2 \frac{\alpha}{\alpha+\beta} \cdot c_s(t) \quad (6)$$

Eq. (6) describes the sap flow of the whole tree as a product of three components: (1) the cross-section area of the tree, which can be considered constant for the time frame of our observations; (2) the shape of the Beta distribution, which, based on our presentation in Part I, can be assumed constant among trees and over time (or subjected to seasonal or annual variability, at least); and (3) a scaling factor c_s that incorporates all the short-time variability in sap velocity and sap flow. In the following analysis, we will demonstrate that c_s is directly linked to hourly and daily shifts in environmental conditions.

2.2. Experimental site

Our experimental site was located in the Morgan–Monroe State Forest (MMSF) in Indiana, USA (39°19′N, 86°25′W). The vegetation at the site is characterized by a secondary successional broadleaf forest with 29 identified species in the immediate vicinity of an eddy covariance tower (Schmid et al., 2000). A survey conducted in 1998 found that 75% of the total basal area was made up of sugar maple (*Acer saccurum*), tulip poplar (*Liriodendron tulipifera*), sassafras (*Sassafras albidum*), white oak (*Quercus alba*), and black oak (*Quercus nigra*), The estimated basal area of sugar maple was 7.14 $m^2\,ha^{-1}$ (Schmid et al., 2000), which was about 27% of the total basal area in the forest. In 2006, the average age of the forest was 80–90 years and the height of the canopy was about 27 m. Leaf area index (LAI) is routinely estimated at several points in the forest and regular intervals for the entire vegetative season, using a LAI-2000 device (LI-COR, Lincoln, NE, USA). Leaf area index in the observation area was constant for the entire measurement period (i.e. at the peak of the vegetative season 2006) at an average of ~4.8 $m^2\,m^{-2}$.

The area has ridge/ravine topography with a relative relief of less than 60 m, and an overall drop of 90 m in 4 km (Schmid et al., 2000); average elevation is about 275 m above sea level. Soils in the area are mesic typic Dystrochrepts dominated by the Berks–Weikert complex, defined as moderately deep and shallow (0.5–1.5 m in the experiment area), steep and very steep, well drained silt-loam formed in residuum from sandstone, siltstone, and shale. This soil association is characteristic of upland areas in this region (Wayson et al., 2006). As a result of the topography and soil properties the soil moisture in the experimental area presents a spatial variability similar to the temporal dynamic observed during a typical vegetative season (Fig. 1a).

Sixteen sugar maples were selected along a ~140 m south-facing topographic transect that spans a relative relief of about 20 m (elevation from 260 to 280 m). The selection of the trees was mostly driven by the necessity to represent the range of diameters at breast height (DBH) observed in the forest. For this reason, the selected trees were spatially distributed over ~80 m in the East–West direction. The topographic transect extended from the top of the hill down to the bottom of the ravine. The DBH range of selected trees was between 11.4 and 31.2 cm. Selected trees did not present any peculiarity in stem and canopy structure, however, three of the smallest trees had canopies that were predominately in the understory.

2.3. Estimating sap velocity

Sap velocity in each tree was estimated using the compensation heat pulse technique (Green et al., 2003; Green and Clothier, 1988) and gauges specifically manufactured for the experiment (Tranzflo NZ LTD, New Zealand). Three different sets of four gauges each were used: the first and the second sets had 2 and 4 cm long probes respectively, and measured sap velocity at four different radial points (depths from the cambium of 0.5, 1.0, 1.5, 2.0 cm and 0.5, 1.2, 2.1, 3.2 cm). These probes were used on the smallest and medium-size trees (less than 20 cm DBH). The third set of probes had 6 cm long needles that measured sap velocity at six radial points (0.5, 1.5, 2.0, 2.5, 3.5, 4.5 and 5.5 cm). These longer probes were used for the largest trees (>20 cm DBH).

The four probes of each set were inserted into each one of the selected trees at breast height, with the four gauges oriented along the magnetic North, East, South and West axes. A metallic plate with pre-drilled holes was used as a guide to drill the three holes and assure a parallel displacement of the probe needles. The upstream and downstream probe needles with thermocouples were vertically placed 20 mm apart, 5 mm below and 15 mm above the heater probe, respectively (Green et al., 2003). Trunk diameters and bark thickness were measured at the location of the gauge installations. Probes

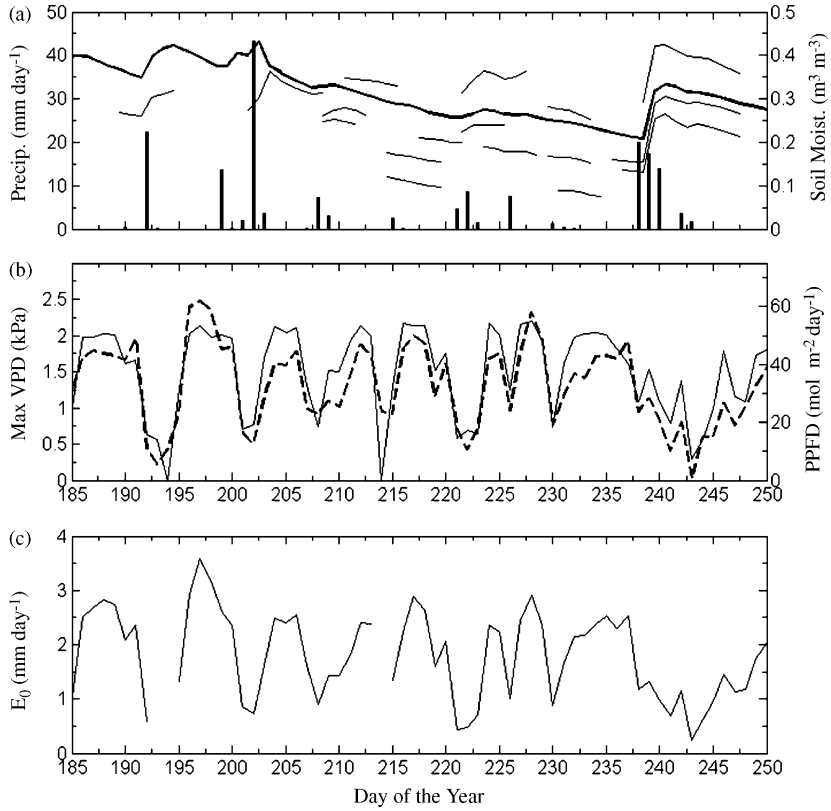

Fig. 1 – Time series of (a) daily total precipitation (solid bar); daily average of soil moisture at sampled tree location (solid line); reference soil moisture (thick solid line); (b) daily maximum VPD (thick-dashed line) and daily total PPFD (solid line); (c) atmospheric transpiration demand (E_0).

were left in place for 5–7 days and then moved to a different tree; thus, only three trees could be measured simultaneously. Heat pulses were released at regular intervals (15 min during the day and 30 min at night). Sap velocities were estimated as described by Green et al. (2003) and Green and Clothier (1988). In particular, a wound size of 2.4 mm was assumed, as suggested by the manufacturer, and the estimated heat pulse velocity (H_V, $L\,T^{-1}$) was converted into sap velocity (v_s, $L\,T^{-1}$) using Becker and Edwards (1999).

$$v_s = H_v(0.441 \cdot F_{wood} + F_{water}), \quad (7)$$

where F_{wood} and F_{water} ($L^3\,L^{-3}$) are estimates of the volume fractions of wood and water, respectively. The wood volume fraction was determined gravimetrically using incremental cores extracted from each tree at the end of the measurement period. Cores were also used to visually determine the depth of the active xylem and sapwood area; when this was not possible or uncertain, the allometric relationship between DBH and sapwood area proposed by Wullschleger et al. (2001) for sugar maple was used. The relationship proposed by Wullschleger et al. (2001) was found to be very similar to the one developed using visual observations (data not shown), and was preferred because it was obtained from a larger number of samples (including trees from the MMSF, Wullschleger et al., 2001).

2.4. *Estimating sap conductance $c_s(t)$*

Measurements of sap flow are required to obtain estimates of stem conductance (Eq. (6)). Interpolation and integration across the radius of the instantaneous sap velocities was accomplished using the Beta distribution function (Eq. (3)) scaled by a factor c as

$$v_s(x,t) = \left[\frac{1}{B(\alpha,\beta)}(x)^{\alpha-1}(1-x)^{\beta-1}\right] \cdot c \quad (8)$$

and maximum likelihood estimates of the parameter α, β, and c for each set of measurements were obtained using the least-square method (Press et al., 2002).

It is important to emphasize that in Eq. (8) no assumption is made about the component $\rho_s(x)$ (like in the case of Eqs. (2) and (3)) and for this reason, the parameter c is a simple fitting coefficient and cannot be interpreted or expected to behave like the stem conductance c_s.

We removed from the analysis any sap velocity profile observation that did not yield coefficients of determination greater than 0.9 (about 13% of the entire daylight dataset and coinciding with low transpiration conditions due to periods of rain or high evaporation rates from the canopy). Instantaneous sap flows measured in each tree were assumed to be constant over the fraction of the cross-section area measured by each probe (i.e. 1/4 if all four probes were functioning). The

algebraic sum of the four fractions provided instantaneous sap flow per tree.

In order to exclude the effects of asynchrony between sap flow and environmental determinants of transpiration (caused, for instance, by changes in stem water capacity) from our analysis, the estimates of potential atmospheric water demand (see next section) were used to determine the time lag between measured sap flow and potential instantaneous transpiration. We adopted the approach proposed by Phillips et al. (1997), by which the daily time series of sap flow and potential atmospheric water demand (E_0) were shifted with increasing time-step to determine the maximum cross-correlation coefficient. Time-shifted sap flow was considered a representative measure of plant transpiration (T_r, $M\,T^{-1}$).

The mean values of α and β distributions (i.e., $\hat{\alpha} = 5.3, \hat{\beta} = 2.0$, see Caylor and Dragoni (2009) and hourly averages of transpiration were used to calculate hourly values of the dynamic component of sap velocity variability c_s under the assumption of a constant $\rho_s(x)$ and by re-arranging Eq. (6) as

$$c_s = \frac{T_r}{2A_s(\hat{\alpha}/\hat{\alpha} + \hat{\beta})} \tag{9}$$

2.5. Potential atmospheric transpiration demand

In order to link stem conductance dynamic to atmospheric water demand, the Jarvis–McNaughton formulation of the Penman–Monteith equation (Jarvis and McNaughton, 1986) was used to estimate the potential atmospheric transpiration demand (E_0, $kg\,m^{-2}\,s^{-1}$) as

$$\begin{aligned} E_0 &= \Omega E_q + (1-\Omega)E_i \\ E_i &= \frac{d_a C_p}{\lambda\gamma} g_l VPD \\ E_q &= \frac{s(R_n - G)}{\lambda(s+\gamma)} \end{aligned} \tag{10}$$

where E_i is the imposed transpiration ($kg\,m^{-2}\,s^{-1}$), E_q the equilibrium transpiration ($kg\,m^{-2}\,s^{-1}$), Ω the transpiration-bulk air coupling factor (unitless), d_a the dry air density ($kg\,m^{-3}$), C_p the specific heat of air at constant pressure ($J\,kg^{-1}\,K^{-1}$), λ the latent heat of vaporization of water ($J\,kg^{-1}$), γ the psychrometric constant ($kPa\,K^{-1}$), g_l the canopy conductance ($m\,s^{-1}$), VPD the atmospheric water vapor pressure deficit (kPa), s the rate of change of saturation water vapor pressure with temperature ($kPa\,K^{-1}$), R_n the net radiation ($J\,m^{-2}\,s^{-1}$), and G is the soil heat flux ($J\,m^{-2}\,s^{-1}$), which we set to 0.1 R_n following Phillips et al. (1997). The omega factor Ω was set to 0.1, a value that represents strong coupling between transpiration control and bulk-air (cf. Jarvis and McNaughton, 1986; Wullschleger et al., 2000). Stomatal conductance was assumed to be constant and equal to 185 $mmol\,m^{-2}\,s^{-1}$ (i.e. about 4.6 $mm\,s^{-1}$). This value of stomatal conductance corresponds to the conductance required to match the average daytime evapotranspiration rate measured by the MMSF eddy-covariance system during the duration of experiment. Using this formulation we necessarily neglect any diurnal variation in stomata conductance associated with cloudy/rainy periods, sunset and sunrise periods, as well as non-stationary changes in leaf physiology (e.g., senescence). In all of these conditions however, transpiration is usually low, which would reduce the amount of error caused by our approximation, and the measurement period did not extend long enough to accommodate changes in tree phenology. Moreover, because our goal is to determine a potential transpiration demand, we feel that the use of a constant stomatal conductance is reasonable.

2.6. Soil moisture availability

Volumetric soil moisture content is routinely measured at the MMSF research site as an average within the upper 30 cm of soil using a single time domain reflectometer buried at 15 cm (TDR, CS615, Campbell Scientific Inc., Logan, UT, USA) at a point about 3/4 downhill of the topographic transect length (Schmid et al., 2000). Observations from this sensor were used as a continuous reference of the overall volumetric soil water content. Also, in order to estimate local water supply from soil (i.e. average of the first 30 cm of depth), a single TDR probe (TDR, CS616, Campbell Scientific Inc., Logan, UT, USA) was installed in proximity (i.e. within 2–3 m) of each sampled tree. These additional probes were previously cross-calibrated under the same soil conditions, using the standard/manufacturer calibration coefficients. The resulting TDR measurements were corrected for soil temperature and for the specific type of soil using coefficients determined from routine weekly gravimetric samples and corresponding measurements of our reference MMSF TDR probe. The relationship developed by Wayson et al. (2006) specifically for the MMSF was used to convert from volumetric water content into soil water potential.

2.7. Sensitivity of c_s to bulk air conditions and water supply and demand

An important consideration is the manner by which stem conductance varies according to shifts in the potential atmospheric water demand (E_0). To examine this relationship, we focus on the slope of the relationship between c_s and E_0, which we define as the sensitivity of c_s to potential atmospheric water demand, S_E ($L^3\,M^{-1}$), given as

$$S_E = \frac{dc_s}{dE_0} \tag{11}$$

Using Eq. (10) to estimate potential atmospheric water demand, we assume that the effects of changes in soil moisture availability on the water status of the trees are negligible and thus, that transpiration is mainly driven by atmospheric water demand. Under such a condition of constant water supply, the value of S_E is also expected to be relatively constant for any individual through time and even between different individuals (e.g., Allen et al., 1998). However, if soil moisture becomes a limiting factor, we expect S_E to change, reflecting the tree's response to the reduced soil water availability. A second assumption implied by the use of E_0 in Eq. (11) is the presence of strong coupling between the rate of transpiration and bulk air conditions. While this is generally the case under most daytime conditions, very low VPD that may occur during and after rain events (i.e. with high evaporation from the canopy) may cause a temporary decoupling between T_r (and c_s) and E_0. For this reason, in

estimating S_E we exclude hours with VPD lower than 0.5 kPa (i.e. 32% of the total number of hours). In addition, we chose to preserve the original units in which c_s and E_0 were estimated (i.e. cm h^{-1} and l m^{-2} of ground area, respectively), in order to avoid uncertainty associated with variables required either to upscale or downscale our measurements (e.g., basal area, leaf area).

2.8. *Landscape scale measurements*

The nearby (i.e. about 200 m downstream the predominant wind direction) MMSF-eddy covariance tower provided all the meteorological observations required for the estimates of the atmospheric transpiration demand, data analysis and result interpretation. All sensors are located at 46 m above ground (about 20 m above canopy) and consist of air temperature/relative humidity (Thermohygrometer VTP37, Meteolabor, Wetzikon, Switzerland), net radiation (CNR1,Kipp and Zonen, Bohemia NY, USA), photosynthetic photon flux density (PPFD, Li-190SA-50, LI-COR, Lincoln, NE, USA), and rain rate (TE525, Texas Eletronics, Dallas, TX, USA). Details regarding this instrumentation are provided in Schmid et al. (2000).

3. Results

The final dataset extended from 5th July to 5th September 2006. Precipitation was occurred throughout the experimental period (Fig. 1a), and totaled 100 mm during the observations, and about 1300 mm for the entire year 2006 (1999–2006 annual average precipitation is about 1000 mm yr^{-1}, unpublished data). Soil moisture ranged from 0.4 m^3 m^{-3} to 0.1 m^3 m^{-3} (i.e. from a soil water potential of about −0.1 to −3.5 MPa), with variability among the sampled tree probes of the same order as the temporal variation recorded by the reference probe (Fig. 1a). As is typical of the study area in mid-to-late summer, water availability in the soil decreased until the end of August, when it sharply increased to pre-drought values after 3 days of rain. We address the large negative soil water potentials observed in our data in Section 4. Maximum daily VPD averaged 1.3 kPa, with peaks of about 2.5 kPa (Fig. 1b). PPFD averaged 37.6 mol m^{-2} day^{-1} with peaks around 55 mol m^{-2} day^{-1} (Fig. 1b). Potential atmospheric water demand followed the patterns of VPD and PPFD, as expected, with daily total values peaking at about 3 mm day^{-1} (Fig. 1c). Estimated time lags between instantaneous transpiration demand E_0 and sap flow F_s were between 20 and 120 min, with a mean of 20 min and no clear patterns related to environmental conditions (e.g., soil water status, or evaporative demand).

Radial profiles of sap velocity follow the same pattern in all our sampled trees, with a sharp increase in the first millimeters after the cambium and a more gradual decline towards the heart/sapwood interface (Fig. 2). Sap velocities peaked at about 45 cm h^{-1} in the small understory trees and 70 cm h^{-1} in the largest trees. Hourly averages of c_s (708 data points in total) were highly variable (Fig. 2, inset), with values peaking up to 15 cm h^{-1} during sunny and hot hours.

Hourly averages of stem conductance (c_s), showed high degrees of linear correlation with the estimated potential atmospheric water demand (average R^2 for all the fits is 0.77, Table 1) and in general, with solar radiation and net radiation (Fig. 3b–d). Linear relationships are also observed between c_s and VPD, but with lower degrees of correlation (Fig. 3a and Table 1). However, c_s sensitivity to bulk air conditions and potential atmospheric water demand (i.e. $S_E = dc_s/dE_0$) varied widely among trees (Fig. 4 and Table 1). In particular, the three relatively small under-canopy trees showed consistently lower values of sensitivity, even compared with the same-size but exposed-canopy trees (Table 1). We excluded the possibility that this sensitivity was induced by the size of the trees (p-value = 0.47 with null hypothesis of $S_E = dS_E/dSWA = 0$, where SWA is individual tree sapwood area). Most likely, the different light and VPD conditions within the understory environment imposed a coupling between transpiration and water supply and demand that has a different dynamic than in the top-canopy trees. For this reason, we

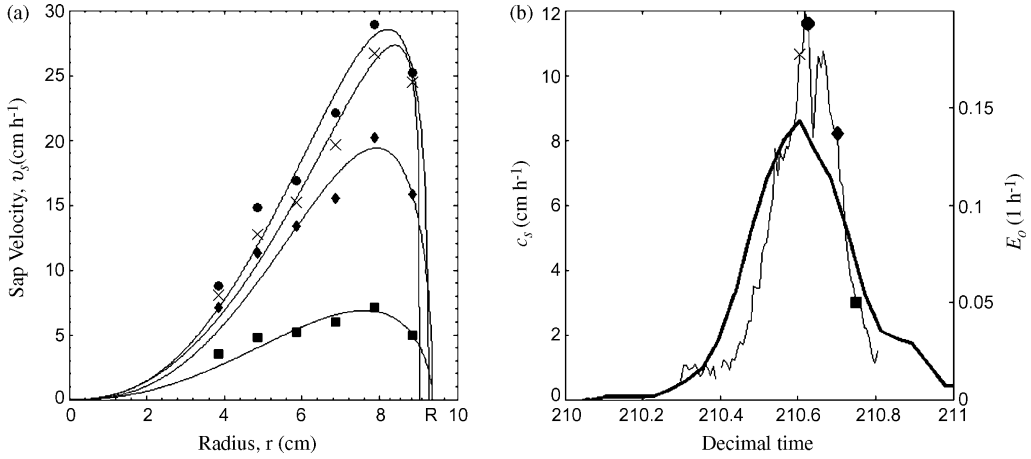

Fig. 2 – (a) Examples of radial sap velocity measurements taken at different hours of the day. Each symbol identifies a different time of the day. Solid lines represent the resulting Beta distributions obtained using the least-square method. (b) Example of daily pattern of the dynamic parameter c_s (Eq. (2)). Similar symbols in both plots associate instantaneous values of c_s with the corresponding sap velocities profiles. Thicker solid line is the atmospheric water demand (E_0) for the same period.

Table 1 – For each sampled tree: diameter at breast height (DBH); average volumetric water content (VWC) for the measurement period; c_s sensitivity to: VPD (S_{VPD}), PPFD (S_{PPFD}), net radiation (S_{Rn}), and potential water demand (S_E). Numbers in parenthesis are the coefficients of determination for the linear regressions, which are all significant with a 95% confidence interval. Understory trees are identified with a asterisk symbol close to the identification number.

Tree #	DBH (cm)	VWC ($m^3\ m^{-3}$)	S_{VPD} (R^2) ($cm\ h^{-1}\ kPa^{-1}$)	S_{PPFD} (R^2) ($cm\ h^{-1}\ \mu mol\ m^{-2}\ s^{-1}$)	S_{Rn} (R^2) ($cm\ h^{-1}\ W\ m^{-2}$)	S_E (R^2) ($cm\ h^{-1}\ mm\ h^{-1}$)
1*	16.3	0.26	5.6 (0.55)	0.0037 (0.54)	0.0083 (0.49)	43.6 (0.87)
2*	5.5	0.32	3.0 (0.63)	0.0017 (0.63)	0.0042 (0.60)	19.4 (0.82)
3	6.7	0.25	7.1 (0.15)	0.0051 (0.77)	0.0132 (0.79)	71.5 (0.74)
4	9.7	0.27	10.5 (0.43)	0.0070 (0.60)	0.0174 (0.57)	81.7 (0.72)
5*	5.4	0.34	2.4 (0.34)	0.0020 (0.55)	0.0048 (0.52)	21.5 (0.65)
6	14.5	0.11	5.0 (0.35)	0.0057 (0.66)	0.0144 (0.63)	45.7 (0.63)
7	7.8	0.17	4.4 (0.41)	0.0041 (0.55)	0.0103 (0.53)	39.7 (0.68)
8	5.3	0.21	5.5 (0.52)	0.0048 (0.66)	0.0121 (0.64)	47.4 (0.83)
9	9.5	0.23	5.5 (0.31)	0.0058 (0.55)	0.0135 (0.54)	64.6 (0.75)
10	15.6	0.35	5.6 (0.37)	0.0054 (0.68)	0.0130 (0.62)	56.3 (0.77)
11	4.8	0.18	2.9 (0.28)	0.0029 (0.41)	0.0071 (0.38)	28.7 (0.50)
12	11.4	0.16	5.0 (0.42)	0.0036 (0.67)	0.0092 (0.65)	42.4 (0.79)
13	12.8	0.27	10.3 (0.34)	0.0078 (0.53)	0.0200 (0.51)	89.6 (0.63)
14	5.7	0.08	5.5 (0.46)	0.0038 (0.65)	0.0096 (0.60)	46.0(0.82)
15	14.8	0.34	10.0 (0.62)	0.0054 (0.31)	0.0132 (0.26)	76.7 (0.73)
16	9.1	0.20	8.2 (0.59)	0.0054 (0.50)	0.0134 (0.46)	67.4 (0.79)

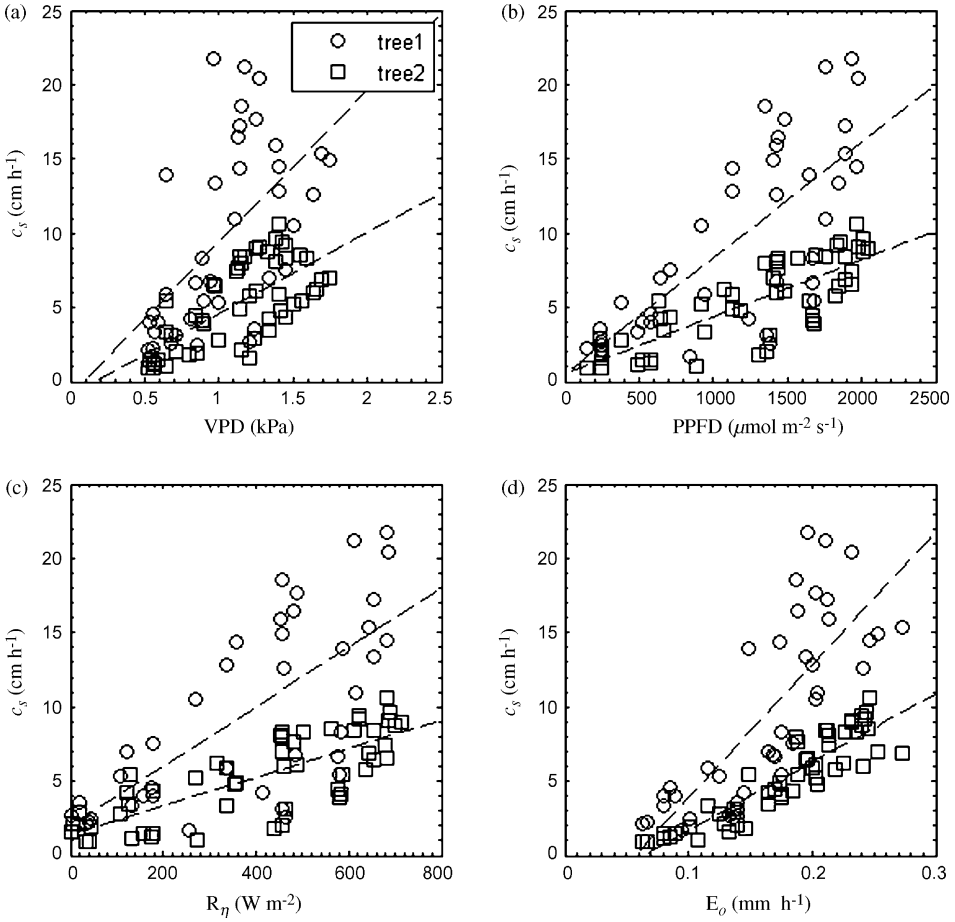

Fig. 3 – Examples of hourly sap velocity variability (c_s, Eq. (9)) from two different trees sampled during the same period of 5 consecutive day; c_s is reported as a function of: (a) vapor pressure deficit (VPD); (b) photosynthetic photon flux density (PPFD); (c) net radiation (R_n) and (d) potential atmospheric water demand (E_0). Dotted lines represent the best linear fits (see also Table 1).

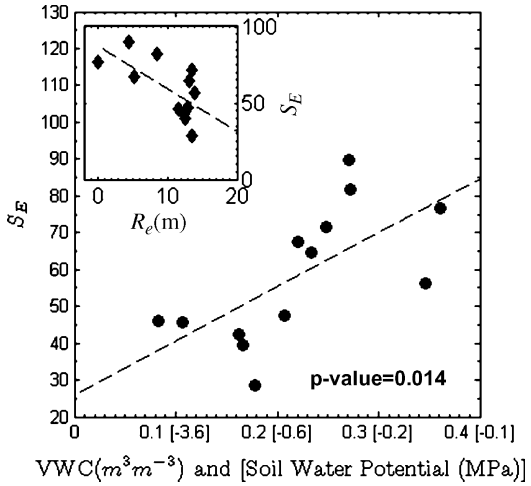

Fig. 4 – Linear regression between the sensitivity of c_s to potential atmospheric water demand (S_E) and average volumetric water content (VWC) and soil water potential (after Wayson et al., 2006) for each sampled tree (R^2 = 0.43, p-value = 0.014). Inset; relation between relative elevation in the topographic transect of each tree (R_e) and γ_E (R^2 = 0.44, p-value = 0.013). Dotted lines describe the resulting linear fit for both datasets.

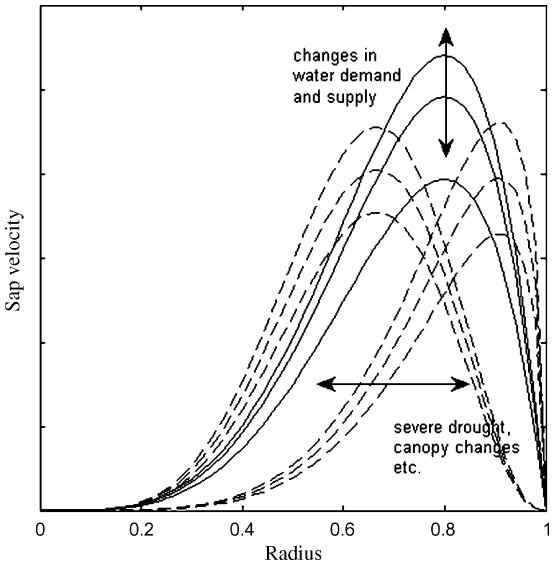

Fig. 6 – Hypothetical mechanism for the responses of radial profiles of sap velocity to environmental, and xylem property changes. Solid lines describe conditions in which the response is mainly mediated by adjustments of transpiration rates at leaf/canopy level (the stem conductance, c_s, in Eq. (2)). Dashed lines describe conditions in which changes in xylem properties occurred as a consequence, for instance, of severe drought, or changes in tree phenology or morphology. Under these conditions, the shape of the sap velocity profile, as described by the parameters α and β of the Beta distribution (Eq. (3)), is different, and the absolute peak value of sap velocity is lower. However, sap velocity is still determined by hourly/daily changes in environmental conditions, like water supply and demand.

excluded the data sets of the three under-canopy trees from further analyses.

Sensitivity of c_s to bulk air conditions and potential atmospheric water demand S_E showed positive correlation with the average soil moisture recorded at each tree (Fig. 5), suggesting that soil water supply had some degrees of control on the transpiration process. However, values of S_E did not show any significant correlation with the soil moisture recorded by the reference probe, located at about 3/4 downhill of the topographic transect length (p-value > 0.4, data not shown); measurements from bottom-of-ravine trees, with higher S_E than concurrent top-of-ravine trees, were the main cause for the low correlation. S_E correlated with the relative distance from the bottom of the ravine (p-value = 0.013, Fig. 5 inset) suggesting that c_s sensitivity to water demand was also driven by the spatial heterogeneity in soil moisture generated by the presence of topography.

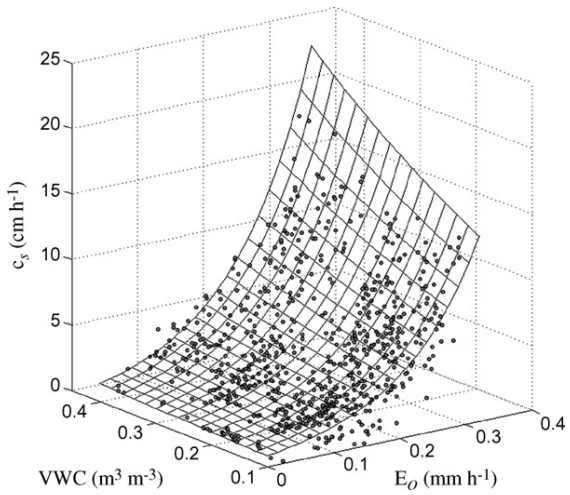

Fig. 5 – Hourly averages of stem conductance c_s as a function of volumetric water content (VWC, proxy for water availability) and potential water demand (E_0). A non-linear model is fitted over the observed data points: $c_s(E_0, VWC) = a \cdot b^{E_0} \cdot c^{VWC}$. The resulting coefficient of determination (R^2) is equal to 0.60, parameter a = 1.01, $b = 9.53 \times 10^{-4}$, c = 4.82.

The entire suite of stem conductance estimates were used in a multiple non-linear regression analysis to develop a general model of c_s variation in response to both potential water demand E_0 and soil moisture as

$$c_s(E_0, \mathrm{VWC}) = a \cdot b^{E_0} \cdot c^{\mathrm{VWC}} \quad (12)$$

Even though the dataset presents a large scatter, the model can explain 60% of the variability of c_s (Fig. 6). Atmospheric water demand is clearly the dominant main driver of variability in stem conductance. However, soil moisture can become a strong secondary limitation on stem conductance, in particular during conditions of high potential water demand

(e.g., 0.3 mm h^{-1}), when c_s difference between moist soil (e.g., 0.40 m^3 m^{-3}) and dry soil (e.g., 0.2 m^3 m^{-3}) can be about 30%.

4. Discussion

While the formulation of Eq. (2) does not exclude the use of any other function to describe the static component of the radial profile of sap velocity, we find that the adoption of the Beta distribution function yielded the best fitting results in our sugar maple samples (coefficients of determination higher than 0.9 for 85% of the hours). These high correlations are likely caused by the Beta distribution function having well-defined boundaries (i.e. it is bounded between 0 and 1) and a shape that is better suited to describing the radial profile of sap velocity than other families of functions such as polynomials or Gaussian curves.

Accordingly to our theoretical framework, the stem conductance c_s is the component of sap velocity that should be directly related to changes in atmospheric water demand and soil water supply. Our results show that c_s is not very strongly correlated with bulk air VPD (average R^2 for all trees = 0.30, Fig. 4a). Instead, we find that PPFD, net radiation (R_n) and potential evaporative demand (E_0) all explain a larger portion of c_s variability (average R^2 = 0.60, 0.57 and 0.73 for PPFD, R_n and E_0, respectively). Our decision to remove hours with VPD <0.5 kPa from the dataset periods may cause a decrease in correlation strength between c_s and VPD, even though a large portion of the rejected hours have transpiration very close to zero (data not shown). In addition, a partial decoupling between bulk air conditions and transpiration process may contribute to lower correlation between stem conductance and VPD (e.g., Wullschleger et al., 2000). However, our results are not affected substantially when the atmospheric VPD measured at 22 m (i.e. inside the top-canopy, where coupling should be stronger) is used instead (data not shown). Nevertheless, prior work has reported weak correlations between radial sap velocity variability and VPD changes (e.g., Ford et al., 2004b; Poyatos et al., 2007), and stronger correlation with the net radiation (Poyatos et al., 2007). Overall, this may suggest that bulk air VPD may not the best variable to describe alone the atmospheric water demand, but rather that VPD should be used in combination with other measures that include net radiation. In this regard, our estimate of potential atmospheric water demand (E_0) shows the strongest correlation with c_s, which indicates strong control of atmospheric water demand on short-term temporal changes in sap velocity. However, as anticipated in Section 3, the intensity of this response differs by tree due to spatio-temporal variation in local soil water supply.

We observe a positive correlation between sensitivity of c_s to potential atmospheric water demand ($S_E = dc_s/dE_0$) and locally measured average soil moisture (Fig. 5). This positive correlation suggests that soil water supply is a limiting factor during a portion of the experiment period and along some portions of our hill slope-scale sampling transect. We do not have direct estimates of soil field capacity and plant wilting point for our experimental site and thus, we cannot directly link variability in S_E to soil properties. However, volumetric water content rarely reaches values above 50% (i.e. soil water potential equal to about −0.04 MPa) at our experimental site, even during the wettest part of the leaf-off season (Ehman et al., 2002). We recognize that the observed minimum soil water potential of −3.5 MPa represents an extreme value for our type of forest, most likely well below the plant wilting point. However, soil water potential values around −3 MPa have been previously observed in temperate forests (Wullschleger and Hanson, 2006), especially in late summer. It is also important to realize that the relationship between volumetric water content and soil water potential in dry soils (Wayson et al., 2006) is highly non-linear and small shifts in volumetric water content cause large changes in soil water potential. For example, in the equation we use here, a change in the estimated water volumetric content from 0.10 m^3 m^{-3} to 0.11 m^3 m^{-3} causes an increase in soil water potential from −3.6 MPa to −2.8 MPa. Furthermore, the lowest values of soil moisture observed in our work (i.e. volumetric water content of about 10%, equivalent to a soil water potential of about −3.5 MPa) are very similar to those observed at the MMSF during the summers of 1999 and 2007, when prolonged droughts caused significant reduction in evapo-transpiration fluxes as estimated by the eddy covariance system (data not shown). The fact that S_E does not demonstrate a clear correlation with the soil moisture measured by the reference probe (data not shown), may indicate that the temporal component of soil moisture dynamics did not impact individual-tree transpiration as much as the spatial component, for which we obtain a strong correlation (i.e. S_E is strongly negatively correlated with tree elevation on the hill slope). However, it is most likely that we are missing part of the correlation between S_E and temporal patterns of soil moisture, due to the short duration of our sap flow measurements, which were taken from each tree for only 5–7 consecutive days. During these shorter sampling periods, the local soil moisture was mostly invariant (Fig. 1a).

Although we observe significant correlations between S_E and both the local soil moisture and the relative tree elevation, the coefficients of determination of the fits are relatively small (0.43 and 0.44 for soil moisture and elevation, respectively). Three factors can explain this result: (1) the use of a single TDR probe per tree is not enough to obtain spatially representative measurements of the average water supply available to each tree; (2) spatially representativeness of TDR probes is also limited by the depth of measurements, which included only the first 30 cm of soil depth, while roots systems have been observed to extend beyond 60 cm of depth at the MMSF (Ehman et al., 2002); (3) the relative tree elevation, although correlated with soil moisture dynamics via lateral soil moisture redistribution, is not as representative of actual soil water availability as, for instance, the topographic index which accounts for local upslope convergence (Western et al., 1999). However, the spatial resolution of available digital elevation data is currently too poor to obtain tree-specific estimates of topographic index or any other measure of local convergence that may affect soil moisture dynamics around individual trees. Therefore, we use the relative elevation as a proxy for soil moisture availability. Another potential source of uncertainty in our results arises from the fact that we estimate potential water demand (E_0) using meteorological observations acquired from the nearby eddy-covariance tower

and therefore are forced to assume spatial uniformity in E_0 across all our sampled trees. For this reason, the effects of variability in microclimate at the individual-tree scale, induced for example by the local topography and canopy structure, are neglected in our approach. Indeed, the large difference between E_0 estimates derived from the tower and the E_0 experienced by understory trees is the reason we excluded them from our S_E analysis. However, for all the other canopy trees we are confident that the relatively mild and short slope, consistent aspect, and consistently high coupling between transpiration and bulk air conditions (Jarvis and McNaughton, 1986; Wullschleger et al., 2000) mitigate heterogeneity in the spatial patterns of potential water demand (E_0) experienced between our sampled trees.

We do not have direct evidence that the actual properties of the xylem (for instance the anatomical characteristics, vessel size, wood density, etc...) do not change in response to short-term environmental fluctuations that occurred during our observational period. In addition, we do not have direct measurements of stomatal conductance from the sampled trees, and are unable to exclude the possibility that the observed variation in S_E may be induced by other factors (e.g., phenology, changes in plant hydraulic resistance, etc...). Nevertheless, our results on both sugar maples and dwarf apple trees (Caylor and Dragoni, 2009) strongly suggest that the interacting effects of soil moisture and atmospheric water demand have no impact on the spatial distribution of sap flowing within the cross-section of the stem (i.e. the shape of the Beta distribution), but instead are directly reflected only in the total sap flow of the tree. However, results from previous studies suggest that this may not be always the case. During a period of severe drought, Cermak and Nadezhdina (1998) observed a substantial reduction in the active sapwood area of a large spruce tree (*Piceas abies*), which led to what the authors define as a "dramatic" change in radial sap velocity pattern. Fiora and Cescatti (2008) reported changes in radial profiles of sap velocity as a consequence of selective pruning in 35-year-old *Picea abies*. Kumagai et al. (2007) also report similar observations to Cermak's in two stand plots of Japanese cedar (*Cryptomeria japonica*) located at the top and bottom of a topographic transect. In Kumagai et al. (2007), trees at the bottom of the slope maintained sap flow at deeper depths into the xylem than trees at the top. However, because trees at the bottom were on average larger, sap flow rates expressed per units of sapwood area resulted in statistically similar values. The results of the first two studies suggest that the shape of the observed radial profiles of sap velocity, as described by the parameters α and β of the Beta distribution function, changed as a result of the severe environmental conditions or manipulation of the canopy structure. In contrast, the report by Kumagai et al. (2007) seems to indicate that the parameters α and β may have remained constant within trees. Ford et al. (2004a) measured sap velocity at two different radial depths in the xylem of *Pinus taeda* and observed diurnal and seasonal variability in the difference between outer and inner flows. However, they also observed that at high fluxes (late morning and afternoon), the difference was more "stable" (Fig. 2 of Ford et al., 2004a). It is not clear if the observed stability during high flux rate indicates the presence of a characteristic radial profile of sap velocity as observed in our sugar maples. Nevertheless, Ford et al. (2004a) reported a clear change in sap velocity profiles with lower soil moisture in some of the observed trees. In particular, under these conditions, "the inner xylem contributed more to total stem flow than under wetter soil". Kubota et al. (2005) applied a Weibull function to interpolate radial sap velocity measurements in three Japanese beech (*F. crenata*) under different environmental conditions that revealed a clear reduction in the absolute peak of sap velocity during cloudy and dry conditions, with a slight shift of the location of peak velocity towards inner xylem during dry conditions. We re-analyzed their results using our Beta distribution approach to estimate the stem conductance and the α and β parameters of the Beta distribution for each of the trees and environmental conditions. Our method yielded R^2 values between 0.92 and 0.94. While we find that stem conductance is highly variable within and among trees, with lower values under cloudy and sunny-dry conditions, our analysis reveals that the shapes of the Beta distribution are very similar and the estimated $\rho_s = \alpha/(\alpha + \beta)$ vary less than 4% for trees under different environmental conditions.

In light of both work regarding variation in radial sap velocities and the detailed analysis we have presented here, we suggest that the properties of the active xylem that determine the shape of the radial profile of sap velocity are not likely to change in response to a wide range of typical environmental conditions to which tree are well-adapted. However, it is also the case that xylem structure and functionality may be greatly altered during periods of severe and/or prolonged droughts as well as in response to substantial changes in tree morphology or phenology, which would affect the shape of the radial profile of sap velocity. This hypothesis is described graphically in Fig. 6 using the Beta distribution; a wide range of sap velocities changes can be explained by the hourly/daily dynamic in stem conductance, with $\rho_s = \alpha/(\alpha + \beta)$ constant. However, during severe and prolonged droughts and changes in tree morphology and/or phenology the peak in sap velocity may be lower, and the outer or inner portions of the xylem may experience a substantial reduction in sap flow. Under these conditions ρ_s is expected to change, although c_s still explains the hourly/daily sap velocity variability.

Based on our observations, we find that sapwood area of our trees (SWA) does not correlate with locally measured soil moisture (S_m, p-value = 0.17 with null hypothesis of $dSWA/dS_m = 0$), which is in contrast to some recent work by Loranty et al. (2008a), who found that sapwood area of individual aspen (*Populu stremuloides*) trees demonstrated a significant spatial correlation with soil moisture. However, Loranty et al. (2008) also predicted that under conditions of soil water supply limitation, the rate of transpiration per unit xylem area could become spatially correlated with soil moisture and drive variability in transpiration of individual trees, which is precisely the dynamics we observed during our observational experiment (cf. Figs. 4 and 5).

5. Conclusions

This research has directly tested the hypothesis proposed in Caylor and Dragoni (2009) that variability in cross-section sap velocity is the product of a time-invariant component

(explained by the parameters α and β of the Beta distribution function and driven by xylem properties) and a dynamic component (explained by the stem conductance, c_s, and driven by both atmospheric water demand and local soil water supply). In particular our work focuses on the link between c_s and water demand and individual tree water supply across a range of conditions where temporal and spatial heterogeneity in environmental conditions are present. Our observations indicate that the stem conductance in sugar maples is (1) strongly correlated with bulk air conditions and potential atmospheric water demand on hourly basis; (2) is independent of tree size; and (3) is also strongly correlated to local soil water availability that arises from the presence of mild topography on relatively shallow soils.

These results provide further confirmation of the approach presented in the companion paper by Caylor and Dragoni (2009). Most critically, they present evidence for a response to changes in water supply and demand that does not necessarily involve changes in the xylem properties and functionality (the α and β parameters of the Beta distribution), but also adjustments of transpiration rates at leaf/canopy level (the stem conductance, c_s). A better understanding of this dynamic response and its environmental determinants is the subject of an ongoing investigation. Because it is likely that the regulation of individual tree responses may be species-specific and linked to both tree age and phenology, our results demonstrate the utility of approaches that seek to characterize the general nature of radial variation in sap velocity when estimating transpiration from point-based sap flow measurements. Ultimately, it is our hope that this work will contribute to advancing ecological studies of tree-scale water use and landscape estimates of transpiration that seek to characterize tree responses to spatio-temporal heterogeneity in both water supply and demand.

Acknowledgements

Primary funding for this research was provided by the Biological and Environmental Research Program (BER), U.S. Department of Energy, through the Midwestern Center of the National Institute for Global Environmental Change (NIGEC) under Cooperative Agreements DE-FC03-90ER61010, DE FG02-03ER63624, and DE-FG03-01ER63278. K. Caylor was also supported by NASA's Interdisciplinary Science Program (NASA-NNG-04-GM71G). Any opinions, findings, and conclusions or recommendations expressed in this publication are those of the authors and do not necessarily reflect the views of the DOE. Access to the MMSF AmeriFlux site is provided by the Indiana Department of Environmental Management, Division of Forestry. K. Caylor acknowledges additional support through a faculty startup grant from Princeton University. We gratefully acknowledge the contributions of Dr. J.C. Randolph for providing tree inventory statistics, Steve Scott, the MMSF Field Crew to the operation and maintenance of the MMSF Flux Tower Facility, and Dr. Alan Lakso (NYSAES, Cornell University) for the use of his sap flow probes. The final version of this manuscript was greatly improved through the comments and suggestions of three anonymous reviewers.

REFERENCES

Allen, R.G., Pereira, L.S., Raes, D., Smith, M., 1998. Crop evapotranspiration: guidelines for computing crop water requirements, FAO Irrigation and Drainage Paper, No. 56, Rome, Italy, xxvi + 300 pp.

Becker, P., Edwards, W.R.N., 1999. Corrected heat capacity of wood for sap flow calculations. Tree Physiol. 19 (11), 767–768.

Bernier, P.Y., Breda, N., Granier, A., Raulier, F., Mathieu, F., 2002. Validation of a canopy gas exchange model and derivation of a soil water modifier for transpiration for sugar maple (*Acer saccharum Marsh.*) using sap flow density measurements. Forest Ecol. Manag. 163 (1–3), 185–196.

Caylor, K.K., Dragoni, D., 2009. Decoupling structural and environmental determinants of sap velocity: Part I. Methodological development. Agric. Forest Meteorol. 149, 559–569.

Cermak, J., Nadezhdina, N., 1998. Sapwood as the scaling parameter defining according to xylem water content or radial pattern of sap flow? Ann. Des Sci. Forest. 55 (5), 509–521.

Ehman, J.L., Schmid, H.P., Grimmond, C.S.B., Randolph, J.C., Hanson, P.J., Wayson, C.A., Cropley, F.D., 2002. An initial intercomparison of micrometeorological and ecological inventory estimates of carbon exchange in a mid-latitude deciduous forest. Global Change Biol. 8 (6), 575–589.

Ewers, B.E., Mackay, D.S., Gower, S.T., Ahl, D.E., Burrows, S.N., Samanta, S.S., 2002. Tree species effects on stand transpiration in northern Wisconsin. Water Resour. Res. 38 (7), 11.

Ewers, B.E., MacKay, D.S., Samanta, S., 2007. Interannual consistency in canopy stomatal conductance control of leaf water potential across seven tree species. Tree Physiol. 27, 11–24.

Fiora, A., Cescatti, A., 2008. Vertical foliage distribution determines the radial pattern of sap flux density in *Picea abies*. Tree Physiol. 28, 1317–1323.

Ford, C.R., Goranson, C.E., Mitchell, R.J., Will, R.E., Teskey, R.O., 2004a. Diurnal and seasonal variability in the radial distribution of sap flow: predicting total stem flow in *Pinus taeda* trees. Tree Physiol. 24 (9), 941–950.

Ford, C.R., McGuire, M.A., Mitchell, R.J., Teskey, R.O., 2004b. Assessing variation in the radial profile of sap flux density in Pinus species and its effect on daily water use. Tree Physiol. 24 (3), 241–249.

Granier, A., 1985. A new method of sap flow measurement in tree stems. Ann. des Sci. Forest. 42 (2), 193–200.

Green, S., Clothier, B., Jardine, B., 2003. Theory and practical application of heat pulse to measure sap flow. Agronom. J. 95 (6), 1371–1379.

Green, S.R., Clothier, B.E., 1988. Water use of kiwifruit vines and apple trees by the heat-pulse technique. J. Exp. Bot. 39 (198), 115–123.

Hatton, T.J., Catchpole, E.A., Vertessy, R.A., 1990. Integration of sapflow velocity to estimate plant water-use. Tree Physiol. 6 (2), 201–209.

Jarvis, P.G., McNaughton, K.G., 1986. Stomatal control of transpiration: scaling up from leaf to region. Adv. Ecol. Res. 15, 1–49.

Jones, H.G., 1992. Energy balance and evaporation, in: Press, C.U. (Ed.), Plants and Microclimate: a Quantitative Approach to Environmental Plant Physiology, New York, pp. 106–130.

Kubota, M., Tenhunen, J., Zimmermann, R., Schmidt, M., Kakubari, Y., 2005. Influence of environmental conditions on radial patterns of sap flux density of a 70-year *Fagus crenata* trees in the Naeba Mountains, Japan. Ann. Forest Sci. 62 (4), 289–296.

Kumagai, T., Aoki, S., Shimizu, T., Otsuki, K., 2007. Sap flow estimates of stand transpiration at two slope positions in a Japanese cedar forest watershed. Tree Physiol. 27 (2), 161–168.

Loranty, M.M., MacKay, D.S., Ewers, B.E., Adelman, J.D., Kruger, E.L., 2008a. Environmental drivers of spatial variation in whole-tree transpiration in an aspen-dominated upland-to-wetland forest gradient. Water Resour. Res. 44, W02441.

Loranty, M.M., Mackay, D.S., Ewers, B.E., Adelman, J.D., Kruger, E.L., 2008b. Environmental drivers of spatial variation in whole-tree transpiration in an aspen-dominated upland-to-wetland forest gradient. Water Resour. Res. 44 (2), 15.

Meinzer, F.C., Clearwater, M.J., Goldstein, G., 2001. Water transport in trees: current perspectives, new insights and some controversies. Environ. Exp. Bot. 45 (3), 239–262.

Oren, R., Phillips, N., Katul, G., Ewers, B.E., Pataki, D.E., 1998. Scaling xylem sap flux and soil water balance and calculating variance: a method for partitioning water flux in forests. Ann. Des Sci. Forest. 55 (1/2), 191–216.

Pausch, R.C., Grote, E.E., Dawson, T.E., 2000. Estimating water use by sugar maple trees: considerations when using heat-pulse methods in trees with deep functional sapwood. Tree Physiol. 20 (4), 217–227.

Phillips, N., Nagchaudhuri, A., Oren, R., Katul, G., 1997. Time constant for water transport in loblolly pine trees estimated from time series of evaporative demand and stem sapflow. Trees Struct. Funct. 11 (7), 412–419.

Poyatos, R., Cermak, J., Llorens, P., 2007. Variation in the radial patterns of sap flux density in pubescent oak (*Quercus pubescens*) and its implications for tree and stand transpiration measurements. Tree Physiol. 27 (4), 537–548.

Press, W.H., Teukolsky, S.A., Vetterrling, W.T., Flannery, B.P., 2002. Numerical Recipes in C: The Art of Scientific Computing. Cambridge University Press, Cambridge, UK; New York.

Schmid, H.P., Grimmond, C.S.B., Cropley, F., Offerle, B., Su, H.B., 2000. Measurements of CO_2 and energy fluxes over a mixed hardwood forest in the mid-western United States. Agric. Forest Meteorol. 103 (4), 357–374.

Smith, D.M., Allen, S.J., 1996. Measurement of sap flow in plant stems. J. Exp. Bot. 47 (305), 1833–1844.

Tang, J.W., Bolstad, P.V., Ewers, B.E., Desai, A.R., Davis, K.J., Carey, E.V., 2006. Sap flux–upscaled canopy transpiration, stomatal conductance, and water use efficiency in an old growth forest in the Great Lakes region of the United States. J. Geophys. Res. 111, G02009, doi:10.1029/2005JG000083.

Wayson, C.A., Randolph, J.C., Hanson, P.J., Grimmond, C.S.B., Schmid, H.P., 2006. Comparison of soil respiration methods in a mid-latitude deciduous forest. Biogeochemistry 80 (2), 173–189.

Western, A.W., Grayson, R.B., Bloschl, G., Willgoose, G.R., McMahon, T.A., 1999. Observed spatial organization of soil moisture and its relation to terrain indices. Water Resour. Res. 35 (3), 797–810.

Wilson, K.B., Hanson, P.J., Mulholland, P.J., Baldocchi, D.D., Wullschleger, S.D., 2001. A comparison of methods for determining forest evapotranspiration and its components: sap-flow, soil water budget, eddy covariance and catchment water balance. Agric. Forest Meteorol. 106 (2), 153–168.

Wullschleger, S.D., Hanson, P.J., 2006. Sensitivity of canopy transpiration to altered precipitation in an upland oak forest: evidence from a long-term field manipulation study. Global Change Biol. 12 (1), 97–109.

Wullschleger, S.D., Hanson, P.J., Todd, D.E., 2001. Transpiration from a multi-species deciduous forest as estimated by xylem sap flow techniques. Forest Ecol. Manag. 143 (1–3), 205–213.

Wullschleger, S.D., Wilson, K.B., Hanson, P.J., 2000. Environmental control of whole-plant transpiration, canopy conductance and estimates of the decoupling coefficient for large red maple trees. Agric. Forest Meteorol. 104 (2), 157–168.